

# New Coupling Scheme for Microstrip Bandpass Filters With Quarter-Wavelength Resonators

Tsung-Nan Kuo, Shih-Cheng Lin, Chi-Hsueh Wang, and Chun Hsiung Chen, *Fellow, IEEE*

**Abstract**—A new coupling scheme for microstrip bandpass filters with quarter-wavelength ( $\lambda/4$ ) stepped-impedance resonators is proposed. In the proposed coupling scheme, two adjacent  $\lambda/4$  stepped-impedance resonators are coupled by directly connecting an admittance inverter between them. By properly designing the connecting position, one may adjust the coupling coefficient between two resonators so that narrow to broad bandwidth filters may easily be fabricated without coupling gaps. Here, the admittance inverter is realized by a  $\lambda/4$  stepped-impedance line. Based on the proposed coupling scheme and the conventional magnetic coupling structure, the filters with narrow or wide bandwidth may be designed and implemented. In addition, folded lines are adopted to make the filter size compact. In this study, a two-pole filter with a 3-dB bandwidth of 5.1% and two four-pole filters with 3-dB bandwidths of 33% and 51% are successfully fabricated. Good agreement between measured and simulated results is observed.

**Index Terms**—Microstrip bandpass filter, quarter-wavelength ( $\lambda/4$ ) resonator, stepped-impedance resonator.

## I. INTRODUCTION

COMPACT-SIZE bandpass filters with a wide range of bandwidth are essential in developing modern microwave communication systems. Recently, planar circuits have become more and more popular due to ease in integration and manufacture, and many microstrip filter structures based on uniform distributed-element resonators have been proposed. For example, quarter-wavelength ( $\lambda/4$ ) resonators have been used to implement the interdigital and combline filters [1]–[4]. In [5], the filters incorporating the stepped-impedance technology with various shaped resonators were reported. However, it is difficult, for the above filters, to realize a wide bandwidth due to the restricted gap width.

Bandpass filters based on half-wavelength ( $\lambda/2$ ) open stubs or  $\lambda/4$  shorted stubs are quite attractive owing to the merits of possessing relatively wide bandwidth and low insertion loss around passband. The optimum distributed high-pass filters [6], [7] using shorted stubs were attractive in the ultra-wideband application; however, the associated design data are only available

for the structures with wider bandwidths. The dual-behavior resonator filter [8] is possible to be designed for various bandpass responses, but it has the drawback of no dc block and the design formulas for obtaining the required specifications are not intuitive. The traditional  $n$ -pole  $\lambda/4$  shorted stub filter [9] is designed according to the characteristic admittances of stubs and connecting lines; hence, it has the difficulty in realizing a filter with narrow bandwidth, because the required stub admittances would be too high to be realized. In [10], the  $\lambda/4$  shorted stubs were used to design narrow to broad bandwidth filters without coupling gaps, but, only the case with uniform stubs were dealt with.

In this study, a new coupling scheme for realizing the narrow-to-broad bandwidth microstrip filters is proposed. By directly connecting an admittance inverter between two stepped-impedance resonators and then suitably designing the connecting position, one may adjust the coupling coefficient between two resonators so that a wide range of coupling may be realized on the planar filter structures. Based on the well-known coupled-resonator approach [9] and the designable coupling coefficients, either narrow- or wide-bandwidth filter using  $\lambda/4$  resonators may be implemented with simple design procedure. Specifically, three microstrip filters with narrow or wide bandwidth are carefully designed and implemented so as to demonstrate the proposed concept.

The proposed coupling scheme to design filters with narrow to broad bandwidths is basically an extension of DiPiazza's work [10], which was never published in a journal and is relatively inaccessible. Although the same principle is used in the design phase, the proposed coupling scheme still has some practical significance because it gives details of the case with nonuniform or stepped stubs and gives details of miniaturization techniques such as using meandered lines.

## II. PROPOSED COUPLING SCHEME USING AN ADMITTANCE INVERTER

The conventional planar coupling schemes, using capacitive-coupled structures or parallel-coupled lines, have some restrictions in achieving a tight coupling. For example, to realize a larger coupling, the separation distance between two capacitive-coupled resonators must be minimized. However, in practice, it is difficult to carry out such a small gap by using the printed circuit board (PCB) fabrication process.

Fig. 1 shows the equivalent schematic of the proposed coupling scheme for which two  $\lambda/4$  stepped-impedance resonators are directly connected or coupled by an admittance inverter. Here, the admittance inverter is represented by a  $J$ -inverter.

Manuscript received May 15, 2008; revised September 10, 2008. First published November 21, 2008; current version published December 05, 2008. This work was supported in part by the National Science Council of Taiwan under Grant NSC 96-2752-E-002-001-PAE and in part by the Excellent Research Projects of National Taiwan University, NTU-ERP-96R0062-AE00-00.

The authors are with the Department of Electrical Engineering and Graduate Institute of Communication Engineering, National Taiwan University, Taipei 106, Taiwan (e-mail: chchen@ew.ee.ntu.edu.tw).

Color versions of one or more of the figures in this paper are available online at <http://ieeexplore.ieee.org>.

Digital Object Identifier 10.1109/TMTT.2008.2007320

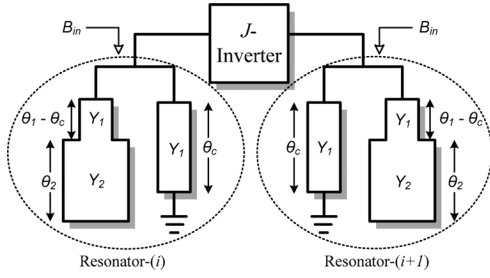


Fig. 1. Equivalent schematic of the proposed coupling scheme for explaining the coupling mechanism.

The mechanism of new coupling scheme in adjusting the coupling coefficient may be explained by calculating the susceptance slope seen into the connecting position. The input susceptance  $B_{in}$  seen into the connecting-position node may be written as

$$B_{in} = \text{Im} \left\{ Y_1 \frac{jY_2 \tan(\theta_2) + jY_1 \tan(\theta_1 - \theta_c)}{Y_1 - Y_2 \tan(\theta_2) \tan(\theta_1 - \theta_c)} - j \frac{Y_1}{\tan(\theta_c)} \right\} \quad (1)$$

and its related susceptance slope  $b_{in}(=b_i)$  can be formulated as

$$b_i = \frac{\omega_0}{2} \left. \frac{\partial B_{in}}{\partial \omega} \right|_{\omega_0} \quad (2)$$

where  $\omega_0$  represents the angular center frequency. Through some manipulations, the relationship between the coupling coefficient  $M_{i,i+1}$  and inverter value  $J_{i,i+1}$  may be established as

$$M_{i,i+1} = \frac{\Delta}{\sqrt{g_i g_{i+1}}} = \frac{J_{i,i+1}}{\sqrt{b_i b_{i+1}}} \quad (3)$$

where  $b_i$  and  $b_{i+1}$  denote the susceptance slopes of resonators  $i$  and  $i+1$ , respectively,  $g_i$  and  $g_{i+1}$  are the element values of lowpass filter prototype, and  $\Delta$  represents the filter fractional bandwidth.

Fig. 2 shows the calculated susceptance slope and coupling coefficient against the connecting position  $\theta_c$ . Here, the numerical values are obtained by using  $Y_1 = 1/93.3 \Omega$ ,  $Y_2 = 1/35 \Omega$ ,  $\theta_1 = \theta_2 = 31.48^\circ$ , and  $J_{i,i+1} = 0.01$ . Note that the susceptance decreases and the coupling coefficient  $M_{i,i+1}$  increases as  $\theta_c$  increases, implying that one may change the coupling by simply adjusting the connecting position. Compared to the conventional planar capacitive-coupled structures, the proposed coupling scheme may realize a wide range of coupling level and largely relieves the restriction due to the printed circuit board fabrication process.

To exemplify the proposed coupling scheme, Fig. 3(a) demonstrates the physical layout of the coupled-resonator pair with an inverter. At this point, the meandered  $\lambda/4$  uniform-impedance line is substituted for the inverter. From the coupled-resonator point of view, the connecting line between two resonators may be considered as a coupling path to provide the required coupling. The full-wave simulated resonance-splitting phenomenon for different  $L_c$  is depicted in Fig. 3(b), where the two split resonance frequencies go remoter as  $L_c$  increases. It is evident that the connecting position may be

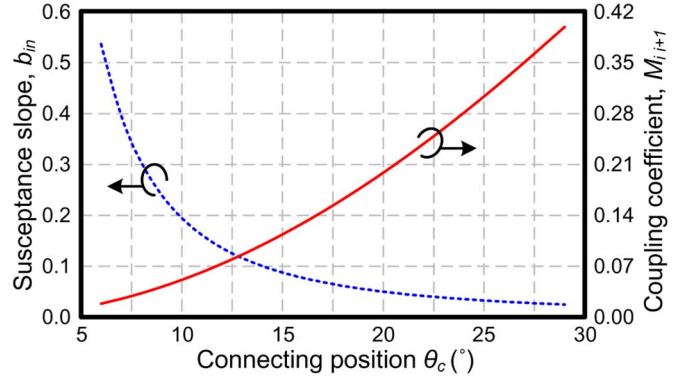


Fig. 2. Calculated susceptance slope and coupling coefficient against the connecting position  $\theta_c$ .

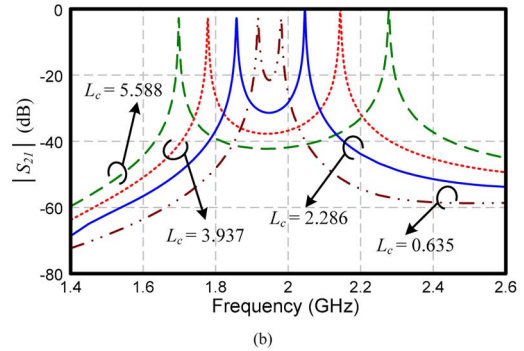
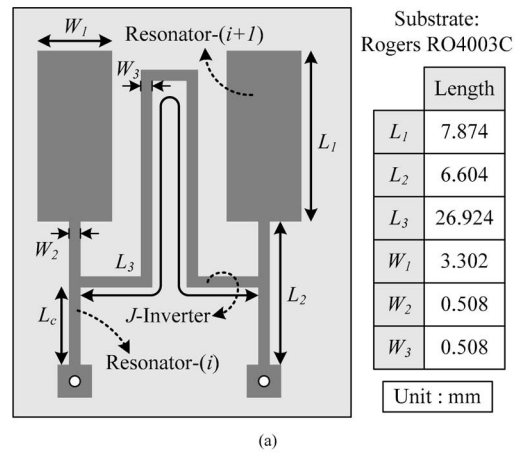


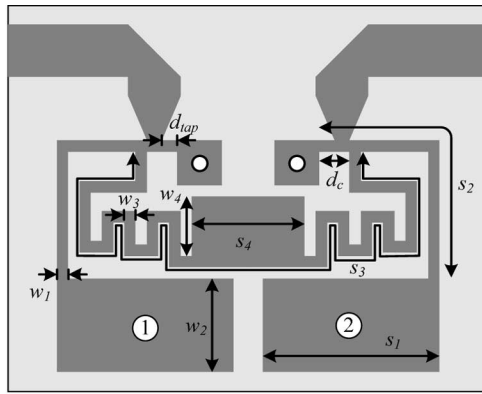
Fig. 3. (a) Physical layout of the coupled-resonator pair with an inverter of meandered  $\lambda/4$  line. (b) Full-wave simulated resonance-splitting phenomenon for different  $L_c$ .

varied to adjust the coupling amount. The coupling coefficient from full-wave simulated results [see Fig. 3(b)] coincides well with the calculated one in Fig. 2.

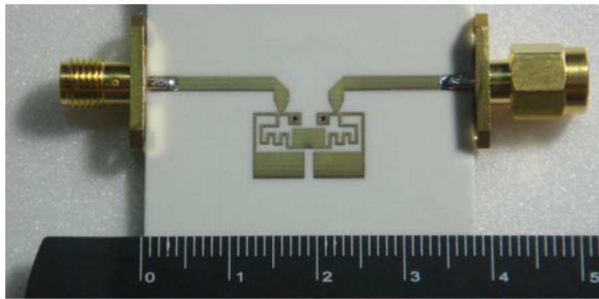
### III. DESIGN PROCEDURES AND REALIZATION OF TWO-POLE FILTER WITH FRACTIONAL BANDWIDTH OF 5%

The well-established coupled-resonator procedures [9] are used to design the proposed filters. Here, several steps are summarized to facilitate the design.

Step 1) Identify the required filter specifications, including the center frequency ( $f_0$ ), fractional bandwidth ( $\Delta$ ), and required low-pass prototype.



(a)



(b)

Fig. 4. (a) Circuit layout and (b) photograph of the proposed two-pole microstrip filter. (Via diameter = 0.508 mm, Via pad =  $1.524 \times 1.524$  mm<sup>2</sup>,  $w_1 = 0.381$  mm,  $w_2 = 3.175$  mm,  $w_3 = 0.381$  mm,  $w_4 = 2.032$  mm,  $s_1 = 5.969$  mm,  $s_2 = 10.287$  mm,  $s_3 = 31.75$  mm,  $s_4 = 3.81$  mm,  $d_{tap} = 0.508$  mm, and  $d_c = 1.016$  mm.).

- Step 2) Decide the impedance ratio and length ratio for the utilized  $\lambda/4$  stepped-impedance resonators. These two parameters determine the occupied resonator size and the spurious passband of overall filter.
- Step 3) Choose the admittance inverter for coupling scheme. Typically, a  $\lambda/4$  uniform-impedance or stepped-impedance line may be adopted as the inverter.
- Step 4) According to the given specifications, determine the connecting position to give the required coupling coefficient  $M_{i,i+1}$ . As mentioned above, for a filter demanding narrow bandwidth, the connecting position associated with the resonators-inverter structure should approach the shorted end of the  $\lambda/4$  resonator, and *vice versa*.
- Step 5) Use the extracting method in [9] to obtain the related external quality factors  $Q_e$ .
- Step 6) To facilitate the overall design, the  $Q_e$  for the utilized tapped-line feeding structure and the coupling coefficient  $M_{i,i+1}$  should be extracted in advance and drawn as design curves with respect to the related positions.

For demonstration, a two-pole filter based on the above-mentioned procedures is fabricated and shown in Fig. 4. Here, the filter is fabricated on the Rogers RO4003C substrate with  $\epsilon_r = 3.38$ ,  $\tan \delta = 0.0022$ , and thickness  $h = 0.813$  mm. The specified center frequency and 3-dB fractional bandwidth are 2 GHz and 5%, respectively. The corresponding coupling coefficient

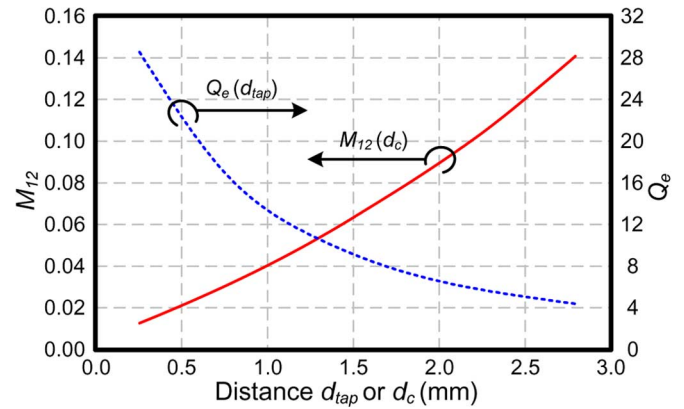


Fig. 5. Design curves concerning external quality factor  $Q_e$  and coupling coefficient  $M_{12}$  for the proposed two-pole filter (Fig. 4).

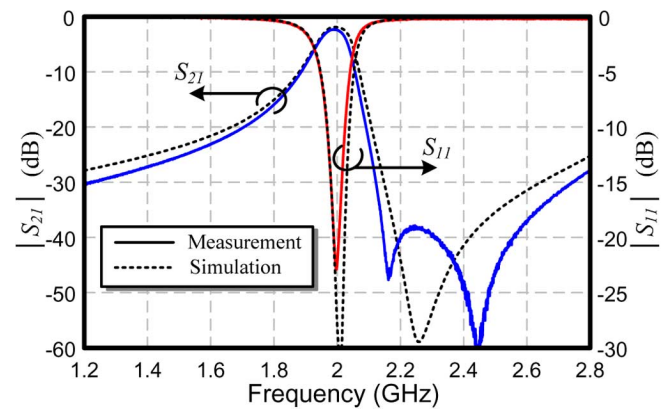


Fig. 6. Simulated and measured frequency responses of the proposed two-pole microstrip filter (Fig. 4) with a 3-dB fractional bandwidth of 5%.

$M_{12}$  converted from the element values of Butterworth low-pass prototype is 0.035, and the external quality factors  $Q_e$  associated with the input/output resonators are 28.284.

To determine the physical dimensions of the filter, the full-wave simulator ADS Momentum is employed to establish the required design curves. As shown in Fig. 5, the design curves relate the coupling coefficient  $M_{12}$  and the external quality factor  $Q_e$  to the distances  $d_c$  and  $d_{tap}$  (see Fig. 4), respectively. Apparently, the connecting position associated with the resonators-inverter structure should be close to the shorted end to get the small quantity of indispensable coupling ( $M_{12} = 0.035$ ). It should be mentioned that the electric length of the inverter must retain  $\lambda/4$  while varying the connecting position for extracting the coupling coefficient. Fig. 6 shows the measured and simulated responses of the narrow-bandwidth two-pole filter shown in Fig. 4. The measured center frequency is at 1.985 GHz and the measured 3-dB fractional bandwidth is 5.1%. The implemented two-pole filter has the insertion loss better than 2.327 dB and a maximum return loss of 22.9 dB. The circuit size of this filter is 7.874 mm  $\times$  12.954 mm, which is approximately  $0.086 \lambda_g \times 0.142 \lambda_g$ , where  $\lambda_g$  is the microstrip guided wavelength on the substrate at center frequency.

By the effect of the open stubs associated with the first and second resonators, a transmission zero around 2.25 GHz is observed in the simulated curve of Fig. 6, because two open-stub

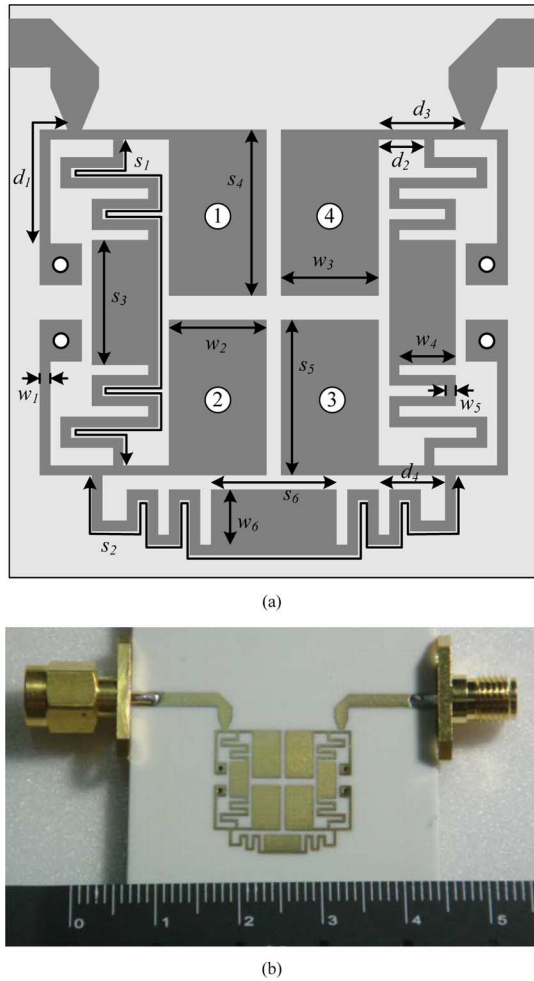


Fig. 7. (a) Circuit layout and (b) photograph of the proposed four-pole microstrip filter using proposed coupling scheme. (Via diameter = 0.508 mm, Via pad =  $1.524 \times 1.524 \text{ mm}^2$ ,  $w_1 = 0.381 \text{ mm}$ ,  $w_2 = 3.556 \text{ mm}$ ,  $w_3 = 3.556 \text{ mm}$ ,  $w_4 = 2.032 \text{ mm}$ ,  $w_5 = 0.381 \text{ mm}$ ,  $w_6 = 2.032 \text{ mm}$ ,  $s_1 = 30.988 \text{ mm}$ ,  $s_2 = 30.48 \text{ mm}$ ,  $s_3 = 4.572 \text{ mm}$ ,  $s_4 = 6.096 \text{ mm}$ ,  $s_5 = 5.715 \text{ mm}$ ,  $s_6 = 4.572 \text{ mm}$ ,  $d_1 = 5.334 \text{ mm}$ ,  $d_2 = 1.651 \text{ mm}$ ,  $d_3 = 3.175 \text{ mm}$ , and  $d_4 = 2.413 \text{ mm}$ ).

lengths are made equal in simulation. However, two transmission zeros are presented in the measured curve, a consequence of unequal open-stub lengths caused by the imperfect fabrication process.

#### IV. REALIZATION OF FOUR-POLE FILTERS WITH WIDE BANDWIDTH

##### A. Four-Pole Filter Using Proposed Coupling Scheme

As mentioned above, compared with the conventional coupled structures, the proposed coupling scheme has an advantage of easily realizing a large coupling amount. To demonstrate this capability, a four-pole filter shown in Fig. 7 with wide bandwidth is fabricated. According to the Chebyshev low-pass prototype, the design parameters for this four-pole filter are determined with the center frequency  $f_0$  at 2 GHz and a 0.1-dB equal-ripple bandwidth of 30%. The external quality factors  $Q_e$  and coupling matrix  $[M]$  associated with the specifications are calculated as

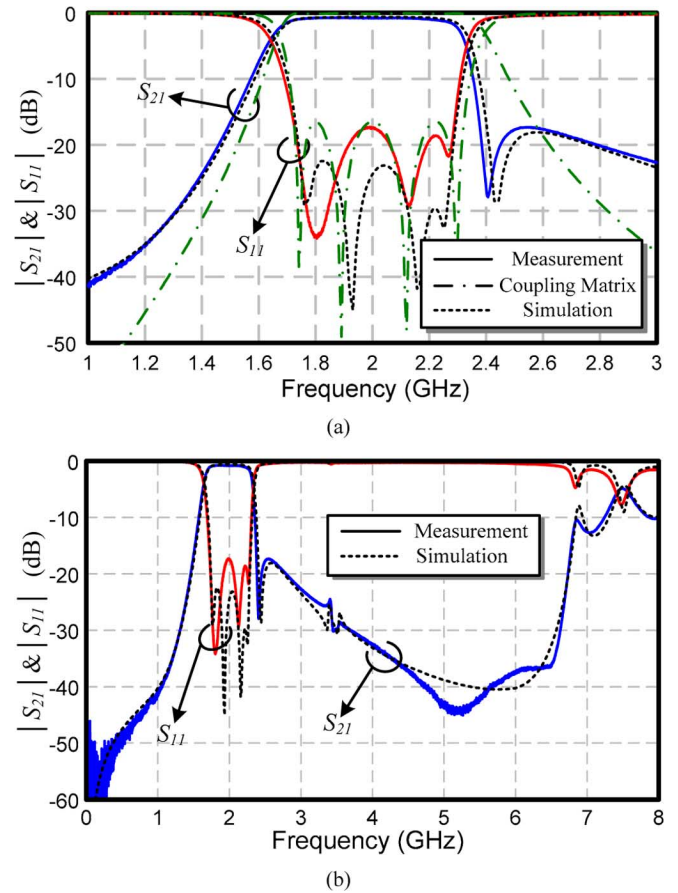


Fig. 8. Simulated and measured frequency responses of the proposed four-pole microstrip filter (Fig. 7) using proposed coupling scheme. (a) Narrowband  $S$ -parameters. (b) Wideband  $S$ -parameters.

$$Q_{ei} = Q_{eo} = 3.696$$

$$[M] = \begin{bmatrix} 0 & 0.2492 & 0 & 0 \\ 0.2492 & 0 & 0.1972 & 0 \\ 0 & 0.1972 & 0 & 0.2492 \\ 0 & 0 & 0.2492 & 0 \end{bmatrix}. \quad (4)$$

The coupling coefficients  $M_{12}$ ,  $M_{23}$ , and  $M_{34}$  are implemented by the proposed coupling scheme. Although there is an extra coupling  $M_{14}$  between the first and fourth resonators, its coefficient  $M_{14}$  is relatively small compared with  $M_{12}$ ,  $M_{23}$ , and  $M_{34}$ , and therefore it will be neglected in the subsequent design. To reduce the circuit size, folded stepped-impedance resonators and meandered lines are arranged to achieve the required coupling. Moreover, by incorporating the steps into inverters, one may shorten the inverter length and suppress the higher order spurious resonances. Like the two-pole filter, the tapped-line coupling is used to get the necessary quality factor  $Q_e$ . Based on this coupling matrix, the theoretical response is calculated and shown in Fig. 8(a).

The measured and simulated responses of the proposed four-pole filter (Fig. 7), which is fabricated on the Rogers RO4003C substrate, are shown in Fig. 8. The implemented four-pole filter has the measured center frequency at 2 GHz, a measured 3-dB fractional bandwidth of 33.08%, a minimum insertion loss of



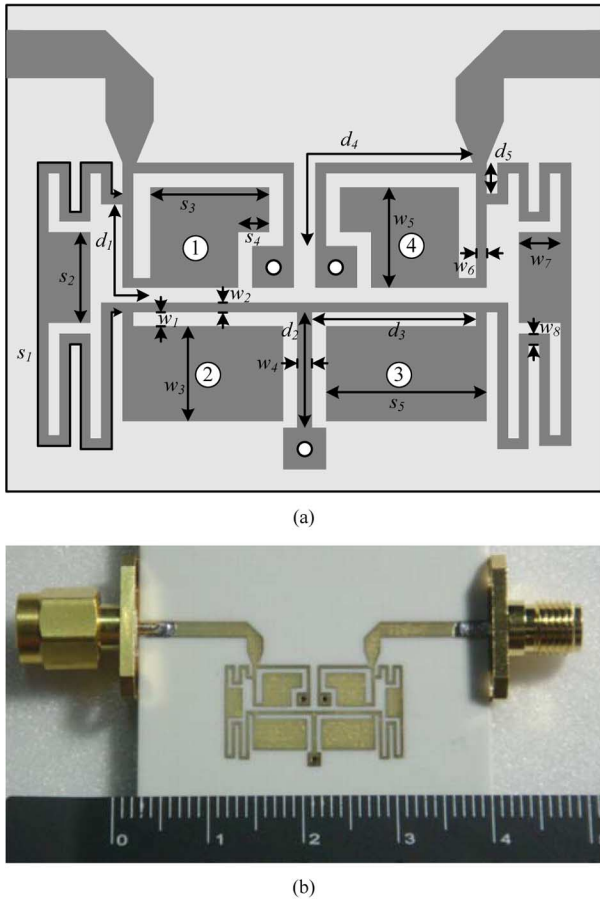


Fig. 9. (a) Circuit layout and (b) photograph of the proposed four-pole microstrip filter using both proposed coupling scheme and magnetic coupling structure. (Via diameter = 0.508 mm, Via pad =  $1.524 \times 1.524 \text{ mm}^2$ ,  $w_1 = 0.508 \text{ mm}$ ,  $w_2 = 0.381 \text{ mm}$ ,  $w_3 = 3.429 \text{ mm}$ ,  $w_4 = 0.508 \text{ mm}$ ,  $w_5 = 3.683 \text{ mm}$ ,  $w_6 = 0.381 \text{ mm}$ ,  $w_7 = 1.524 \text{ mm}$ ,  $w_8 = 0.381 \text{ mm}$ ,  $s_1 = 33.528 \text{ mm}$ ,  $s_2 = 3.302 \text{ mm}$ ,  $s_3 = 4.318 \text{ mm}$ ,  $s_4 = 1.143 \text{ mm}$ ,  $s_5 = 5.824 \text{ mm}$ ,  $d_1 = 4.064 \text{ mm}$ ,  $d_2 = 4.191 \text{ mm}$ ,  $d_3 = 5.969 \text{ mm}$ ,  $d_4 = 8.763 \text{ mm}$ , and  $d_5 = 1.143 \text{ mm}$ ).

0.77 dB, and a return loss of 17.28 dB. This fabricated four-pole filter has a compact dimension of  $15.621 \text{ mm} \times 17.018 \text{ mm}$ , which is approximately  $0.172\lambda_g \times 0.187\lambda_g$ .

The transmission zero generated by the open stub associated with the first or fourth resonator is again observed around 2.407 GHz in Fig. 8. With this transmission zero, the selectivity of the upper stopband is improved. Note that the full-wave simulated result is not fully agreed with the theoretical response synthesized by the coupling matrix. The deviation can be contributed to the generation of transmission zero which is not included in the coupling matrix. It may also be contributed to the variations in the coupling coefficients and external quality factors between simulated and theoretical cases.

#### B. Four-Pole Filter Using Both Proposed Coupling Scheme and Magnetic Coupling Structure

Among various planar coupling schemes, the magnetic coupling using a shunt inductance is a desirable candidate for realizing a large amount of coupling coefficient. Hence, for the sake of reducing via-holes and circuit size, the required strong magnetic coupling is implemented by a common shorted stub

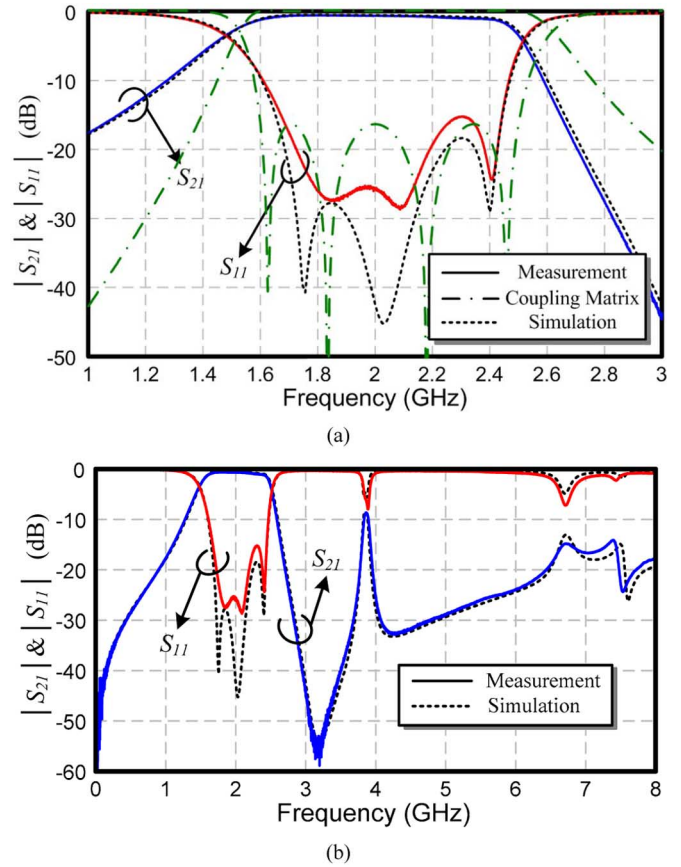


Fig. 10. Simulated and measured frequency responses of the proposed four-pole microstrip filter (Fig. 9) using both proposed coupling scheme and magnetic coupling structure. (a) Narrowband  $S$ -parameters. (b) Wideband  $S$ -parameters.

for the second and third coupled-resonators. Fig. 9 exhibits the physical layout of the four-pole filter with a wider bandwidth. Similarly, all stepped-impedance resonators and lines are folded for size reduction.

According to the Chebyshev low-pass prototype, this filter is designed with the center frequency  $f_0$  at 2 GHz and a 0.1-dB equal-ripple bandwidth of 45%. By these design specifications, the external quality factors  $Q_e$  and coupling matrix  $[M]$  may be written as

$$Q_{ei} = Q_{eo} = 2.464$$

$$[M] = \begin{bmatrix} 0 & 0.3739 & 0 & 0 \\ 0.3739 & 0 & 0.2959 & 0 \\ 0 & 0.2959 & 0 & 0.3739 \\ 0 & 0 & 0.3739 & 0 \end{bmatrix}. \quad (5)$$

The large coupling coefficients  $M_{12}$  and  $M_{34}$  are achieved by the proposed coupling scheme while the strong magnetic coupling  $M_{23}$  is realized by the common shorted stub associated with the second and third resonators. Note that the longer the common shorted stub, the larger the magnetic coupling established. The theoretical response transformed from this coupling matrix is also given in Fig. 10(a).

The measured and simulated responses of the proposed four-pole filter (Fig. 9), which is again fabricated on the Rogers RO4003C substrate, are shown in Fig. 10. The implemented four-pole filter has the measured center frequency at 1.99 GHz,

a measured 3-dB fractional bandwidth of 51.62%, a minimum insertion loss of 0.656 dB, and a return loss of 15.2 dB. This fabricated four-order filter with only three via-holes has a compact size of 11.176 mm  $\times$  19.304 mm, which is approximately  $0.123 \lambda_g \times 0.212 \lambda_g$ .

## V. CONCLUSION

In this paper, a new coupling scheme for microstrip filters with  $\lambda/4$  stepped-impedance resonators has been proposed. By introducing an admittance inverter between two  $\lambda/4$  coupled resonators and suitably designing the connecting position, one may realize a coupled structure with wide range of coupling coefficients, thereby enabling narrow to broad bandwidth filters to be implemented without coupling gaps. Specifically, three microstrip filters based on the proposed coupling scheme, a two-pole filter with narrow bandwidth and two four-pole filters with wide bandwidth, have been successfully designed and fabricated. The new coupling scheme realizes a filter not only with wide range of bandwidth but also with symmetric structure, compact size, and good performance. The proposed filters are suitable for the progressive microwave communication applications with assorted bandwidths.

## REFERENCES

- [1] G. L. Matthaei, "Interdigital bandpass filters," *IEEE Trans. Microw. Theory Tech.*, vol. MTT-10, no. 7, pp. 479–491, Jul. 1962.
- [2] J. S. Wong, "Microstrip tapped-line filter design," *IEEE Trans. Microw. Theory Tech.*, vol. MTT-27, no. 1, pp. 44–50, Jan. 1979.
- [3] D. G. Swanson, "Narrow-band microwave filter design," *IEEE Micro*, pp. 107–114, Oct. 2007.
- [4] E. G. Cristal, "Tapped-line coupled transmission lines with application to interdigital and combline filters," *IEEE Trans. Microw. Theory Tech.*, vol. 23, no. 12, pp. 1007–1012, Dec. 1975.
- [5] M. Sagawa, M. Makimoto, and S. Yamashita, "Geometrical structures and fundamental characteristics of microwave stepped-impedance resonators," *IEEE Trans. Microw. Theory Tech.*, vol. 45, no. 7, pp. 1078–1085, Jul. 1997.
- [6] W. T. Wong, Y. S. Lin, C. H. Wang, and C. H. Chen, "Highly selective microstrip bandpass filters for ultra-wideband (UWB) applications," in *Proc. Asia-Pacific Microw. Conf.*, Nov. 2005, pp. 2850–2853.
- [7] J. G. Garcia, J. Bonache, and F. Martin, "Application of electromagnetic bandgaps to the design of ultra-wide bandpass filters with good out-of-band performance," *IEEE Trans. Microw. Theory Tech.*, vol. 54, no. 12, pp. 4136–4140, Dec. 2006.
- [8] A. Manchec, C. Quendo, E. Rius, C. Person, and J.-F. Favennec, "Synthesis of dual behavior resonator (DBR) filters with integrated low-pass structures for spurious responses suppression," *IEEE Microw. Wireless Compon. Lett.*, vol. 16, no. 1, pp. 4–6, Jan. 2006.
- [9] J. S. Hong and M. J. Lancaster, *Microstrip Bandpass Filters for RF/Microwave Applications*. New York: Wiley, 2001, ch. 8, pp. 151–155.
- [10] G. C. DiPiazza, "Transmission line type microwave filter," U.S. Patent 3,345 589, Dec. 14, 1967.



**Tsung-Nan Kuo** was born in Taoyuan, Taiwan, in 1981. He received the B.S. degree in electrical engineering from National Dong Hwa University, Hualien, Taiwan, in 2003, and the M.S.E.E. and Ph.D. degrees from National Taiwan University, Taipei, Taiwan, in 2005 and 2008, respectively.

His research interests include the design and analysis of microwave filter circuits.



**Shih-Cheng Lin** was born in Taitung, Taiwan, in 1981. He received the B.S. degree in electrical engineering from National Sun Yet-Sen University, Kaohsiung, Taiwan, in 2003, and Ph.D. degree from National Taiwan University, Taipei, Taiwan, in 2007.

His research interests include the design and analysis of microwave filter circuits.



**Chi-Hsueh Wang** was born in Kaohsiung, Taiwan, in 1976. He received the B.S. degrees in electrical engineering from National Cheng Kung University, Tainan, Taiwan, in 1997, and Ph.D. degree from National Taiwan University, Taipei, Taiwan, in 2003.

He was a Post-Doctoral Research Fellow with the Graduate Institute of Communication Engineering, National Taiwan University. His research interests include the design and analysis of microwave and millimeter-wave circuits and computational electromagnetics.



**Chun Hsiung Chen** (SM'88–F'96) was born in Taipei, Taiwan, on March 7, 1937. He received the B.S.E.E. degree in electrical engineering from National Taiwan University, Taipei, Taiwan, in 1960, the M.S.E.E. degree from National Chiao Tung University, Hsinchu, Taiwan, in 1962, and the Ph.D. degree in electrical engineering from National Taiwan University in 1972.

In 1963, he joined the Faculty of the Department of Electrical Engineering, National Taiwan University, where he is currently a Professor. From August 1982 to July 1985, he was Chairman of the Department of Electrical Engineering, National Taiwan University. From August 1992 to July 1996, he was the Director of the University Computer Center, National Taiwan University. In 1974, he was a Visiting Scholar with the Department of Electrical Engineering and Computer Sciences, University of California at Berkeley. From August 1986 to July 1987, he was a Visiting Professor with the Department of Electrical Engineering, University of Houston, Houston, TX. In 1989, 1990, and 1994, he visited the Microwave Department, Technical University of Munich, Munich, Germany, the Laboratoire d'Optique Electromagnetique, Faculte des Sciences et Techniques de Saint-Jerome, Universite d'Aix-Marseille III, Marseille, France, and the Department of Electrical Engineering, Michigan State University, East Lansing, respectively. His areas of interest include microwave circuits and computational electromagnetics.